Fine-structure excitation of CCS by He: Potential energy surface and scattering calculations

A Godard Palluet, François Lique

Accepted to J. Chem. Phys. 10.1063/5.0138470

Fine-structure excitation of CCS by He: Potential energy surface and scattering calculations

A. Godard Palluet[1] and F. Lique[1]
Université de Rennes 1, CNRS, IPR (Institut de Physique de Rennes) - UMR 6251, F-35000 Rennes, France

(*Electronic mail: amelie.godard@univ-rennes1.fr)

(*Electronic mail: francois.lique@univ-rennes1.fr)

(Dated: 5 January 2023)

The fine structure excitation of the interstellar CCS radical induced by collisions with He is investigated. The first potential energy surface (PES) for the CCS-He van der Waals complex is presented. It was obtained from a highly correlated spin unrestricted coupled cluster approach with single double and perturbative triple excitations [UCCSD(T)]. The PES presents two shallow minima of 31.85 and 37.12 cm^{-1} for the linear (He facing S) and the nearly T-shaped geometries, respectively. The dissociation energy of the complex was calculated and found to be $D_0 = 14.183$ cm^{-1}. Inelastic scattering calculations were performed using the Close-Coupling approach. Cross sections for transitions between the 61 first fine structure levels of CCS were obtained for energy up to 600 cm^{-1} and rate coefficients for the 5 - 50 K temperature range were derived. This set of collisional data can be used to model CCS emission spectra in dark molecular interstellar clouds and circumstellar enveloppes and enable an accurate determination of CCS abundance in these astrophysical media.

I. INTRODUCTION

In 1984, a new emission line at 45.379 GHz was detected in TMC-1, TMC-2 and SgrB2 by Suzuki *et al.*,[1] but remains unidentified due to its atypical shape explained by an extraordinary large spin-splitting.[1] At that time, it was the most intense unassigned line among radio lines,[1,2] suggesting that the observed molecule is one of the most abundant species in molecular clouds.[3] This mysterious line was finally assigned to the CCS($^3\Sigma^-$) radical a few years later by Saito *et al.*[3]

After this detection, astronomers started to look for longer carbon chains containing sulfur, now convinced that they exist in space.[4] Hence, C_nS (n = 3, 4, 5) chains were detected in several astronomical sources.[2,5–9] Researchers also started to investigate the formation processes of these carbon chains. Different mechanisms were discussed for decades,[10–20] and still are. Their main production pathways are thought to involve ion-neutral reactions forming HC_nS^+, followed by its dissociative recombination.[10–14,17,20] It was also proposed that these carbon-chains can be formed and can grow through neutral-neutral reactions involving C_nS or H_mC_nS (m, n = 1, 2) molecules.[15–20] In addition, proofs were reported that sulfur-containing carbon chains chemistry is related to the one of nitrogen-containing carbon-chains.[14,21]

After its first assignement, CCS was widely observed in dark molecular clouds, including TMC-1.[2,4,14,21–28] It was also seen in the circumstellar envelope of IRC+10216,[6,29] in the protostellar envelope of B335,[25] and in Bok globules.[30]

The CCS molecule is a key to understand the physical and chemical evolution of molecular clouds.[14,20,24,25] Its abundance is highly sensitive to physical conditions, and thus reflects some properties that are hidden by other tracers.[24] Indeed, it is produced in dense gas as a result of the collapse of the core, and it is rapidly destroyed in the densest material of the central region. Its distribution will thus describe the variation of physical conditions of the observed molecular clouds.[24] Therefore, its abundance ratio with NH_3, which will be desorbed from grain surface during star formation, indicates evolution stages of dense cores[14,23,27] and Bok globules.[30] In addition, the CCS lines are intense enough to investigate physical structures of dense cores,[23] such as clumps and dense filaments, which are suggested to play a dominant role in the formation of prestellar cores.[26,28] Finally, due to its fine structure, CCS can also be used to estimate the magnetic field in molecular clouds by measuring the Zeeman splitting of its lines.[31,32]

A reliable modeling of chemical species abundances from emission spectra requires accurate collisional data.[33] Collisional excitation in molecular clouds and circumstellar envelope (astrophysical media where CCS molecules are mostly detected) are mainly induced by H_2 and He. Such accurate collisional data do not exist yet for CCS to the best of our knowledge. In fact, due to the presence of an electronic spin, and a large spin-splitting, CCS very peculiar internal structure (see Section II B) can only be described with the intermediate coupling scheme as presented by Alexander & Dagdigian,[34] which makes the accurate collisional data quite difficult to compute.[25]

In radiative tranfer models involving CCS, three sets of approximate collisonal data were used. Fuente *et al.*[21] and Suzuki *et al.*[14] computed CCS-H_2 rate coefficients using the OCS-H_2 rotational rate coefficients of Green & Chapman,[35] to which they reintroduced the spin dependence with the Infinite Order Sudden (IOS) approximation. Wolkovitch *et al.*[25] computed CCS-H_2 rotational rate coefficients based on OCS-H_2 PES of Green & Chapman[35] with the Close-Coupling (CC) approach. The spin dependence was also reintroduced with the IOS approximation. However, the IOS approximation used to compute all these sets of collisional data, is considered not to be suitable for molecules presenting large spin-splitting such as CCS.[21,25,36,37] Note that in all these calculations, H_2 was considered as a structureless projectile.

The aim of this work is to overcome this lack of accurate CCS collisonal data by providing the first state-to-state rate coefficients for the CCS-He collisional system considering explicitely the fine structure levels of CCS.

To this end, a new highly correlated PES of the CCS-He system was computed. It was then used in scattering calculations using a close-coupling (CC) approach to provide the dissociation energy of the complex and fine structure resolved rate coefficients for the 5 - 50 K temperature range. The collisional data that we provide here could be used to derive accurate abundances of the CCS molecule in dark molecular clouds and circumstellar envelope such as TMC-1 and IRC+10216, respectively.

Section II presents the computational methods used to obtain the PES (Sec.II A), a description of the peculiar fine structure of the CCS ($^3\Sigma^-$) radical (Sec. II B), the methods used to compute the dissociation energy of the complex (Sec.II C), and scattering data (Sec.II D).

In Section III the results of the calculations are presented. The new PES is described in Section III A. The dissociation energy D_0 of the complex and the effect of the fine structure on its computed value is discussed in Section III B. Accurate fine-structure resolved collisional rate coefficients based on cross sections are presented in Section III C. Finally, the rate coefficients are compared to the latest set of CCS-H_2 data provided by Wolkovitch *et al.*[25] in Section III D.

II. METHODS

A. CCS-He potential energy surface (PES)

1. *ab initio calculations*

In its ground electronic ($^3\Sigma^-$) and vibrational states, the CCS molecule is linear.[38,39] The interaction potential between CCS and He was described using Jacobi coordinates (R,θ), where R is the distance between the center of mass of the CCS radical and the He atom, and θ describes the angle between **R** and CCS internuclear axis (see Figure 1). The internuclear distances in the CCS radical were set at their experimental equilibrium distances r_{C-S} = 2.96a_0 and r_{C-C} = 2.47a_0.[4]

The potential energy surface (PES) was computed with the spin unrestricted coupled-cluster single double and perturbative triple excitations *ab initio* method [UCCSD(T)][40] and the augmented correlation consistent quadruple-zeta basis set (hereafter aVQZ) augmented by additional mid-bond functions of Cybulski & Toczylowski.[41]

The *ab initio* calculations have been performed for 32 values of θ between 0 and 180° with an unregular step. For each value of θ, 44 values of R were chosen between 4.5 and 30a_0 with various steps in order to accuratly describe the different range of interactions. All *ab inito* points were computed with the MOLPRO package.[42]

The basis set superposition error was corrected at every geometry (R, θ) with the counterpoise procedure of Boys & Bernardi:[43]

$$V(R,\theta) = E_{CCS-He}(R,\theta) - E_{CCS}(R,\theta) - E_{He}(R,\theta) \quad (1)$$

where $V(R,\theta)$ is the interaction potential, and all energies E are computed with full basis set.

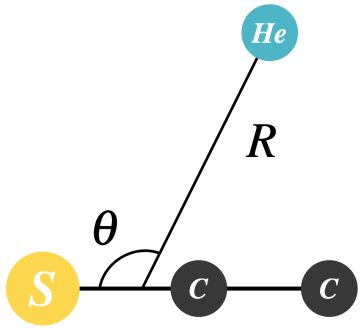

FIG. 1. Representation of the CCS-He collisional system in Jacobi coordinates.

2. *Analytical representation*

A global fit of the interaction potential $V(R,\theta)$ was performed based on the 1351 *ab initio* points using an expansion over Legendre polynomials $P_\lambda(cos\theta)$.[44]

$$V(R,\theta) = \sum_{\lambda=0}^{\lambda_{max}} v_\lambda(R) P_\lambda\ (cos\theta) \quad (2)$$

where λ_{max} was taken equal to 31 according to the number of θ angles calculated. The radial coefficients $v_\lambda(R)$ have been fitted following the procedure of Werner *et al.*[44] The long-range of interaction was fitted and extrapolated using a multipolar expansion with $\frac{C_n}{R^n}$ (n = 6, 8 and 10) coefficients. The fitted potential reproduces all of our *ab initio* points with an error inferior to 1.7%. The root mean square (RMS) deviation is equal to 3.51 cm^{-1} but is mostly due to deviations at short distances for angles between 140 and 180° where the PES is highly repulsive. The RMS is about 0.016 cm^{-1} in the potential well regions ($V(R,\theta)$ < -1 cm^{-1}), and about 9.3 $\times$ 10^{-4} in the long-range of interactions ($0 \leq V(R,\theta) \leq$ -1 cm^{-1}).

B. Fine structure of CCS

In $^3\Sigma^-$ open-shell molecules, as CCS in its electronic ground state, a coupling between the electronic spin S and the rotational angular momentum of the radical N occurs. This so-called spin-rotation coupling will split the rotational levels into fine structure levels. CCS energy levels are described with an intermediate coupling representation.

The total angular momentum j is then expressed as:

$$\mathbf{j} = \mathbf{N} + \mathbf{S} \quad (3)$$

In the intermediate coupling scheme for $S = 1$, the rotational wavefunction can take 3 expressions for each $j \geq 1$ as:[34,45,46]

$$\begin{aligned} |F_1 jm\rangle &= cos\alpha|N = j-1, Sjm\rangle + sin\alpha|N = j+1, Sjm\rangle, \\ |F_2 jm\rangle &= |N = j, Sjm\rangle, \\ |F_3 jm\rangle &= -sin\alpha|N = j-1, Sjm\rangle + cos\alpha|N = j+1, Sjm\rangle, \end{aligned} \quad (4)$$

where $|N, Sjm\rangle$ denotes pure Hund's case (b) basis functions, and α is the mixing angle. This angle is obtained by diagonalization of the molecular Hamiltonian. It depends on j, on the rotational constant B_0, on the spin-rotation constant γ_0, and on the spin-spin constant λ_0.

In pure Hund's case (b) limit, $\alpha \to 0$ and the F_1, F_2 and F_3 fine structure levels will correspond to $N = j$ - 1, $N = j$, and $N = j + 1$, respectively.

Hereafter, each fine structure energy level will be labeled as for pure Hund's case (b) by the couple of quantum numbers N_j according to the astrophysical notation.

The rotational and fine energy levels of the CCS radical were computed with the use of McGuire *et al.*[47] spectroscopic constants: $B_0 = 0.216074$ cm^{-1}; $D = 5.760985 \times 10^{-8}$ cm^{-1}; $\gamma_0 = -4.907061 \times 10^{-4}$ cm^{-1}; $\lambda_0 = 3.242098$ cm^{-1}. Fine structure levels of CCS are represented in Figure 2. For CCS, the fine structure levels are ordered by their rotational quantum number N only from $N_j \geq 10$. For N values from 1 to 10, α decreases from 41 to 17°, exhibiting the decreasing degree of coupling between pure Hund's case (b) basis as N increases.

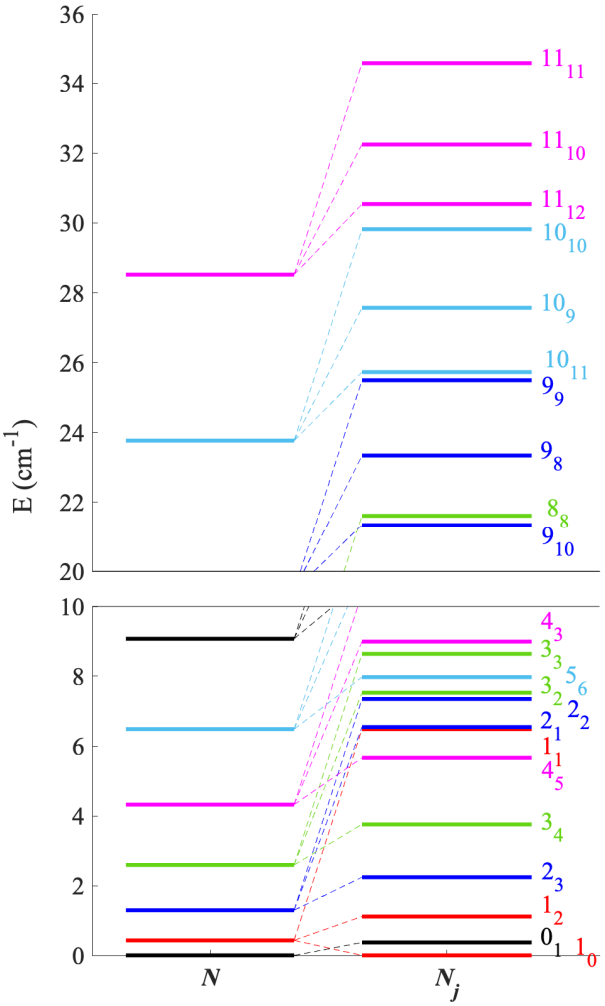

FIG. 2. Representation of the rotational (left) and fine structure (right) energy levels of the CCS($^3\Sigma^-$) radical.

C. Dissociation energy calculations

The dissociation energy D_0 of the $^{12}C^{12}C^{32}S$-He complex was obtained from the new highly correlated PES using the coupled-channel approach. The coupled-equations were solved with the log-derivative method of Manolopoulos[48] as implemented in the BOUND software.[49]

Calculations were performed both with only the rotational structure of CCS (e.g. neglecting the spin-rotation and spin-spin couplings), and then considering the fine structure of CCS. As the fine structure of CCS is peculiar, it might be expected to observe some impact on the bound state energies and thus on the dissociation energy, if the fine structure is taken into account or not.

The parameters were adjusted in order to converge de dissociation energy to better than 0.0001%. For the calculations with the rotational structure alone, the rotational basis contains the first 23 rotational levels (up to N = 22). The propagation parameter R_{max} and DR were set to 56a_0 and 0.004, respectively. To accurately include the fine structure of CCS, a modified version of the BOUND software was used.[49] The basis contains the first 64 fine structure levels (up to $N_j = 21_j$). The propagation parameter R_{max} and DR were set to 36a_0 and 0.014, respectively.

D. Scattering calculations

1. *Cross sections and rate coefficients calculations*

As previously mentioned, the CCS radical is often found in cold molecular clouds. The temperature in these astrophysical media varies from few to a few of tenth of K.[50] CCS was also detected in the outer part of B335 circumstellar envelope, where the temperature is about 25 K[24] and in the outer part of IRC+10216 circumstellar envelope in which the temperature is typically around 50 K.[29]

In astrophysical media, only levels with an internal energy ≤ 100 cm^{-1} can be considered as significantly populated at 50 K. Scattering calculations were thus performed for fine structure levels up to $N_j = 20_j$, with the 20_{20} fine structure level at 96.79 cm^{-1}.

To ensure the convergence of the cross sections for the range of temperature of interest, the scattering calculations

E (cm^{-1})	N_{max}	J_{max}	R_{max}	STEPS	DNRG
0.5 - 30	18	26	30	65	0.5
30 - 50	21	31	20	40	0.5
50 - 100	27	40	20	25	0.5
100 - 150	29	46	20	20	0.5
150 - 200	31	51	14	16	1
200 - 300	32	59	14	12	1
300 - 400	35	64	14	12	2
400 - 500	37	71	14	12	2
500 - 600	39	76	14	11	2

TABLE I. MOLSCAT parameters used in the scattering calculations. the energy step DNRG used to span the energy grid is also given.

were performed for transitions between the first 61 fine structure levels for a total energy E up to 600 cm^{-1} with a various energy step in order to accurately describe their resonances.

Accordingly, all calculations reported in the present paper were carried out by taking into account the exact energy splitting of the levels as well as rotational wavefunction that are linear combination of pure Hund's case (b). Inelastic cross sections from an initial state N_j to a final one $N'_{j'}$ are given by:[34]

$$\sigma_{N_j \to N'_{j'}} = \frac{\pi}{(2j+1)k^2_{N_j}} \times \sum_{jll'} (2J+1) |\delta_{N_j N'_{j'}} \delta_{jj'} \delta_{ll'} - S^J(N_j l; N'_{j'} l')|^2 \quad (5)$$

with $k^2_{N_j} = \frac{2\mu}{\hbar^2}[E - E_{N_j}]$. E is the total energy of the system, and E_{N_j} is the energy of the N_j level.

The scattering matrices $S^J(N_j l; N'_{j'} l')$ were computed for each total energy E with the Close-Coupling (CC) approach and the log-derivative propagator of Manolopoulos[48] implemented in the MOLSCAT code.[51]

Some parameters were constrained by the fit of the PES. Hence, the minimum distance of propagation of the wavefunction R_{min} = 4.36a_0, allowing the calculations up to 1500 cm^{-1}, and λ_{max} = 31, the number of radial coefficients used to describe the PES. Some of the parameters were obtained through convergence tests. Hence, STEPS related to the step of propagation of the wavefunction, R_{max} the largest distance of propagation of the wavefunction and N_{max} the highest rotational quantum number of CCS included in the basis were adjusted. The total angular momentum J_{max} of the system was automatically converged by the MOLSCAT code. These parameters, that can be found in Table I, were converged to ensure less then 2% of uncertainties on the cross sections.

Rate coefficients are computed assuming a Maxwell-Boltzmann distribution of kinetic energies, as:

$$k_{N_j \to N'_{j'}}(T) = \left(\frac{8k_B T}{\pi\mu}\right)^{1/2} \left(\frac{1}{k_B T}\right)^2 \int_0^\infty E_k \sigma_{N_j \to N'_{j'}}(E_k) e^{-E_k/k_B T} dE_k, \quad (6)$$

with k_B the Boltzmann constant.

III. RESULTS AND DISCUSSIONS

A. PES

The isocontours of the PES produced in this work are presented in Figure 3. It was computed with the UCCSD(T)/aVQZ level of theory with additional mid-bond functions, as described in Section II A. The PES has one local minimum V = - 31.85 cm^{-1} for the linear complex (θ = 0°), with the He atom facing the sulfur of the CCS radical at R = 8.35 a_0 , and a global minimum at V = - 37.12 cm^{-1} for the nearly T-shaped complex (θ = 97.72°) at R = 6.70 a_0. These two minima are separated by a low barrier of about 16 cm^{-1} with respect to the global minimum.

The PES is globally highly anisotropic with respect to the θ coordinate, which explains why 32 angular coefficients were needed to obtain its correct analytical fit. Nonetheless, if θ is considered only between 0° and ∼ 100°, i.e. when the He atom is attracted by the sulfur side of CCS, then the anisotropy is not very pronounced. On the contrary, if θ is considered between 100° and 180°, the He is approaching CCS while facing the terminal carbon and the interaction is highly repulsive.

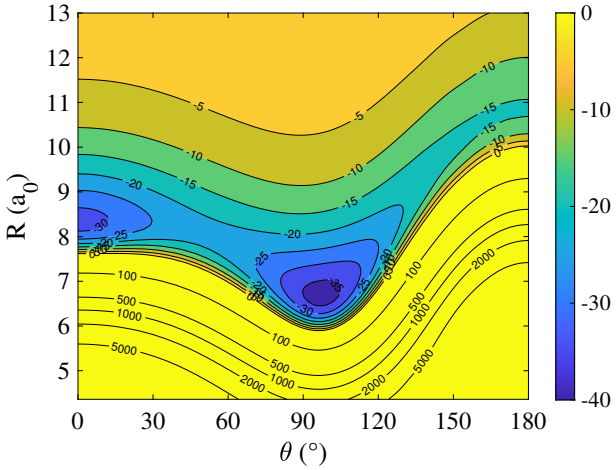

FIG. 3. Isocontours (in cm^{-1}) of the CCS-He PES.

B. Dissociation energy calculations

The dissociation energies, with only the rotational structure of CCS included and with the fine structure of CCS taken into account, were computed based on the methodology described in Section II C.

If the fine structure is neglected, then the computed dissociation energy D_0 is 14.159 cm^{-1}. If the fine structure is taken into account, then D_0 = 14.183 cm^{-1}. In both cases, the dissociation energy is found above the barrier between the two minima of the complex.

The good agreement between these two results, different by less then 0.2%, demonstrates that the fine structure, even if peculiar, does not have a strong influence on D_0, the dissociation

energy of the complex, contrarily to what could have been anticipated. This agreement shows that the coupling between the electronic spin of CCS and the rotation of the whole complex is weak. However, this difference is not negligible, and could be probed by experimental measurements. Thus, the impact of the fine structure on the dissociation energy D_0 value is moderated, but still, the fine structure needs to be taken into account for calculations of spectroscopical accuracy.

To the best of our knowledge, no measurements of the dissociation energy for the CCS-He complex have been reported. However, the comparison between theoretical and future experimental measurements could help us evaluating the quality of the PES. The PES could also be used to study the spectroscopy of the complex. Indeed, such calculations are sensitive to the shape and the depth of the potential wells since it is where bound states are located and can also be another probe of the PES quality.

C. Cross sections and rate coefficients

In this section, cross sections obtained from the scattering calculations performed as detailed in Section II D 1 are presented. Rate coefficients, which are derived from averaging these cross sections over a Boltzmann distribution of the velocities, are also described.

In Figures 4 and 5, cross sections as a function of kinetic energy are presented in the upper panels, and their associated rate coefficients as a function of temperature are in the lower panels. These collisional data are represented for $\Delta N = \Delta j$ (F_i conserving) transitions, which are the dominant ones.

In the cross sections of both figures, Feshbach and shape resonances are observed when the kinetic energy is lower or similar to the well depth, so when $E_k \lesssim 37$ cm^{-1}. These are explained by the temporary formation of (quasi)bound states.[52] These resonances have to be taken into account in order to obtain correct values and behaviors of the rate coefficients, especially at low temperatures, and it justifies why the energy step needed to be smaller when the collisional energy is small or similar to the well depth of the PES.

As one can see, the same type of transitions are represented within the lowest N_j levels (from the $N_j = 1_j$ levels) in Fig. 4, so when fine structure levels are not ordered by increasing N values, and within $N_j \geq 10_j$ levels (from the $N_j = 10_j$ levels) in Fig. 5, so when they are ordered by increasing N values. If low-N_j fine structure levels are considered (Fig. 4), then the rate coefficients with the same ΔN but with different j (different F_i) have very different magnitudes. In fact, they can differ by up to 2 orders of magnitude. At the opposite, if high-N_j transitions are considered (Fig. 5), then, the rate coefficients for transitions with the same ΔN are very similar. Therefore, it is suspected that the strength of the mixing between Hund's case (b) basis have a huge influence on the rate coefficients and on the propensity rules.

To discuss this hypothesis, propensity rules are investigated in Fig. 6 where rate coefficients from $N_{j=N+1} = 1_2$, 6_7 and 10_{11} levels as a function of ΔN are represented at 30 K. Different initial level were considered since, according to Figs. 4 and 5, the propensity rules are expected to change with respect to the initial N_j levels.

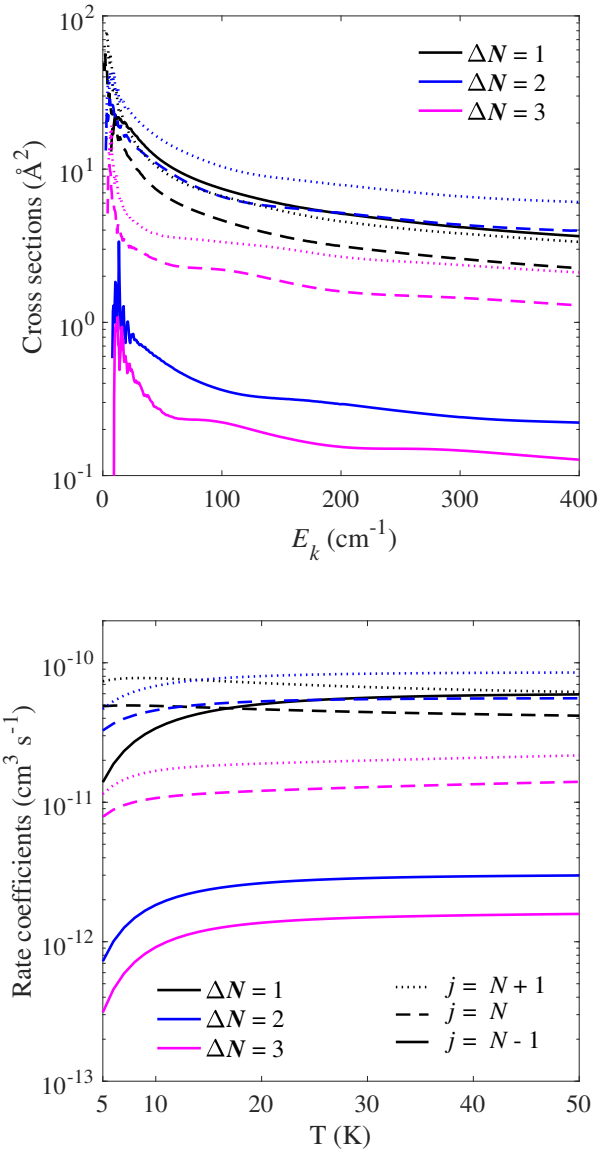

FIG. 4. Cross sections as a function of kinetic energy (upper panel) and rate coefficients as a function of temperature (lower panel) for $\Delta N = \Delta j$ transitions from the 1_j levels.

For all transitions, rate coefficients globally decrease with increasing ΔN. However, the general propensity rule is in favor of transitions with even ΔN compared to transitions with odd ΔN. It was already observed in other ($X^3\Sigma^-$) systems, for which it was justified by the even anisotropy of the PES.[36,46,53–56] The propensity rule favouring even ΔN fades with increasing ΔN, and it tends to vanish when $\Delta N \geq 10$, where the magnitude of the rate coefficients then only de-

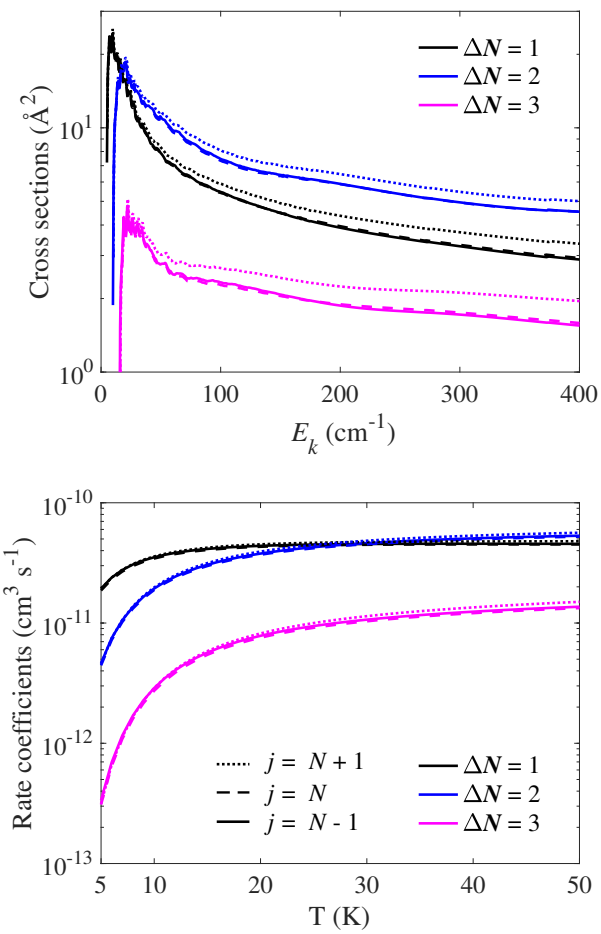

FIG. 5. Cross sections as a function of kinetic energy (upper panel) and rate coefficients as a function of temperature (lower panel) for $\Delta N = \Delta j$ transitions from the 10_j levels.

crease with increasing ΔN following the exponential energy-gap behavior.

As previously mentioned, $\Delta N = \Delta j$ transitions are dominant compared to other type of transitions. This behavior is frequently observed in molecules in ($X^3\Sigma^-$) electronic state,[36,46,53,54,57–59] and was also predicted by Alexander & Dagdigian.[34] The latter study also mentioned that this propensity rule is independent of the degree of intermediate coupling. However, a competition between $1_2 \rightarrow N_{j=N+1}$ (F_1 conserving) and $1_2 \rightarrow N_{j=N-1}$ ($F_1 \rightarrow F_3$) transitions for $\Delta N \geq 10$ is observed in the left panel and is in conflict with Alexander & Dagdigian[34] prediction.

To understand this surprising behavior, the wavefunctions of the different 1_2, 6_7 and 10_{11} initial states considered here are presented according to equations (4):

$$\begin{aligned} 1_2 &\equiv 0.75|1_2\rangle + 0.66|3_2\rangle \\ 6_7 &\equiv 0.92|6_7\rangle - 0.40|8_7\rangle \\ 10_{11} &\equiv 0.96|10_{11}\rangle - 0.29|12_{11}\rangle \end{aligned}$$

With regard of the wavefunction expressions, it can be observed that the level hitherto named 1_2 is actually a linear combination of the $|1_2\rangle$ and the $|3_2\rangle$ Hund's case (b) basis with similar weight. As N increases, for a $N_{j=N+1}$ (F_1) level, the weight of the $|N = j-1, Sjm\rangle$ basis increases, and the weight of the $|N = j+1, Sjm\rangle$ basis decreases. Thus, as N increases, the internal structure of the system tend to be closer to a pure Hund's case (b) description.

Therefore, when one of the state involved in the transition cannot be represented within a pure Hund's case (b) (as for the 1_2 level), then usual Hund's case (b) propensity rules are not valid anymore. At the opposite, when the levels can be reasonably described by a pure Hund's case (b) approach (as for the 10_{11} level), the expected propensity rules for pure Hund's case (b) are then valid.

Alexander & Dagdigian[34] also predicted $\Delta N = \Delta j$ for $j = N$ (F_2 conserving) transitions to be dominant, and $\Delta N = \Delta j$ for $j = N + 1$ (F_1 conserving) and for $j = N - 1$ (F_3 conserving) to be equal. However, for CCS-He rate coefficients, $\Delta N = \Delta j$ for $j = N + 1$ (F_1 conserving) transitions are the most dominant ones for low N_j levels, and all $\Delta N = \Delta j$ transitions tend to be equivalent for high N_j levels, as show in Figure 5.

The relative magnitude of $N_{j=N+1} \rightarrow N_{j=N}$ ($F_1 \rightarrow F_2$) and $N_{j=N+1} \rightarrow N_{j=N-1}$ ($F_1 \rightarrow F_3$) transitions depends here on the N_j initial level. Indeed, when transitions from the 10_{11} fine structure level are considered (right panel), rate coefficients for transitions to final $N_{j=N}$ (F_2) levels are stronger than transitions to final $N_{j=N-1}$ (F_3) levels. This propensity rule corresponds to Hund's case (b) limit, in agreement with previous observation that levels with $N_j \geq 10$ are well described within pure Hund's case (b). However, this propensity rule reverses when N of the initial level decreases. For transitions from the 6_7 (F_1) fine structure level (center panel), transitions to final $N_{j=N-1}$ (F_3) and $N_{j=N}$ (F_2) are in competition. For transitions from the 1_2 (F_1) fine structure level (left panel), rate coefficients for transitions to final $N_{j=N-1}$ (F_3) levels are stronger than rate coefficients to final $N_{j=N}$ (F_2) levels. This propensity rules do not correspond to Hund's case (b) limit,[34] and can be explained by the fact that the mixing between Hund's case (b) basis is significant for low N_j levels. Such findings clearly confirm that the mixing between pure Hund's case (b) levels is not negligible for the CCS($^3\Sigma^-$) molecule, and thus, that a pure Hund's case (b) approach will not be suitable for this system.

D. Comparison with previous data

In this part, our rate coefficients are compared to the most recent ones provided by Wolkovitch *et al.*,[25] in order to evaluate the potential impact of the new collisional data on the modeling of CCS observations.

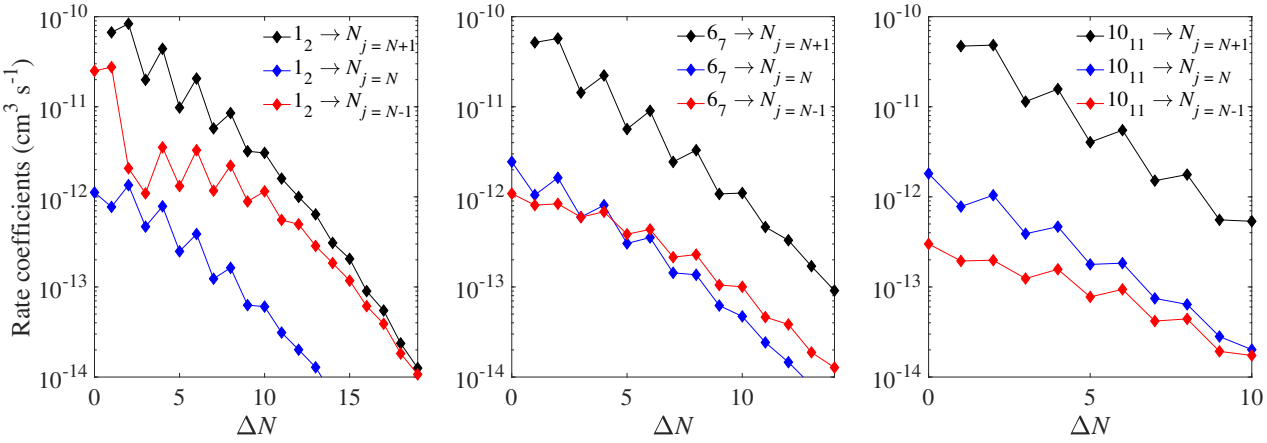

FIG. 6. Propensity rules for transitions out of the 1_2 (left panel), 6_7 (center panel) and 10_{11} (right panel) levels for a temperature of 30 K.

Wolkovitch *et al.*[25] rate coefficients were obtained for fine structure levels up to $N_j = 12_j$ based on OCS-H_2 PES of Green & Chapman.[35] This PES was adapted from an OCS-He interaction potential computed with the electron gas model. As mentioned in the introduction, the H_2 collider is thus considered as a structureless particle, as done for the He atom in this work. Based on this PES, Wolkovitch *et al.*[25] computed rotational rate coefficients with the CC approach, to which they reintroduced the spin-dependence with the IOS approximation within the pure Hund's case (b), as developed by Corey & McCourt.[60]

In Fig. 7, a comparison between fine-structure rate coefficients computed by Wolkovitch *et al.*[25] and in the present work is done at 10 and 20 K.

A difference of a factor 2-10 is globally found between the two sets of rate coefficients at both temperature considered. The distribution around the $x = y$ axis is very sparse, and differences up to 2 orders of magnitude are observed for some transitions at both 10 and 20 K.

For astrophysical modeling, it was found that an order of magnitude of difference in collisional excitation rate coefficients can induce up to a factor 2–5 in the abundance determinations.[33] Therefore, the differences between the two sets of rate coefficients are very significant and should impact the determination of CCS abundances in astrophysical media.

The discrepancies between Wolkovitch *et al.*[25] set of data and the one presented in this work are the results of the different projectiles, of the different PESs, and of the use of different scattering approaches (the IOS approximation within pure Hund's case (b) description of the levels is used in Wolkovitch *et al.*[25] work).

In order to investigate the influence of the PES and of the different colliders, pure rotational rate coefficients were computed from the new CCS-He PES presented in Section III A. The scattering calculations were performed with the CC approach to obtain converged cross sections for the first 13 rotational CCS energy levels for temperatures up to 20 K. Rotational rate coefficients from the ground rotational state are compared in Table II to the ones used by Wolkovitch *et al.*[25]

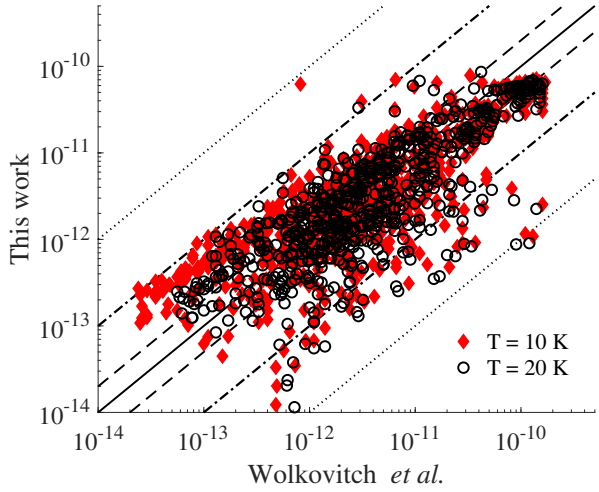

FIG. 7. Direct comparison of Wolkovitch *et al.*[25] CCS-H_2 fine-structure resolved rate coefficients and CCS-He ones provided in this work at 10 K (red diamonds) and 20 K (black open circles). The solid line represents a perfect agreement between the two sets of data; dashed, dashed-dotted and dotted lines delimit the regions where the rate coefficients differ by less than a factor of 2, 10 and 100, respectively.

to derive their fine-structure resolved rate coefficients.

For the dominant transitions, i.e. for transitions with even ΔN, the agreement between these rates is better than a factor of 2, especially at 10 K where the agreement for these transitions for $\Delta N \leq 6$ are better than 20%. The differences between the rotational rate coefficients increase as the ΔN increases, in particular at 10 K, where it reaches almost 2 orders of magnitudes for $\Delta N = 12$. However, such small rate coefficients do not significantly contribute to the fine structure rate coefficients within the IOS approach used by Wolkovitch *et al.*[25] At 20 K, the discrepancies stay under a factor of 2 for all transitions with $\Delta N \leq 10$. If the discrepancies between rotational

	T = 10 K		T = 20 K	
$N \rightarrow N'$	Wolkovitch *et al.*[25]	This work	Wolkovitch *et al.*[25]	This work
$0 \rightarrow 1$	4.8×10^{-11}	9.82×10^{-11}	4.5×10^{-11}	8.90×10^{-11}
$0 \rightarrow 2$	1.1×10^{-10}	9.77×10^{-11}	1.1×10^{-10}	1.08×10^{-10}
$0 \rightarrow 3$	2.2×10^{-11}	2.41×10^{-11}	2.0×10^{-11}	2.59×10^{-11}
$0 \rightarrow 4$	5.8×10^{-11}	5.90×10^{-11}	5.8×10^{-11}	7.21×10^{-11}
$0 \rightarrow 5$	1.5×10^{-11}	7.96×10^{-12}	1.4×10^{-11}	1.10×10^{-11}
$0 \rightarrow 6$	2.0×10^{-11}	1.92×10^{-11}	1.8×10^{-11}	3.41×10^{-11}
$0 \rightarrow 7$	1.3×10^{-11}	3.40×10^{-12}	1.0×10^{-11}	7.03×10^{-12}
$0 \rightarrow 8$	1.1×10^{-11}	4.14×10^{-12}	9.5×10^{-12}	1.31×10^{-11}
$0 \rightarrow 9$	7.6×10^{-12}	8.79×10^{-13}	6.1×10^{-12}	3.65×10^{-12}
$0 \rightarrow 10$	8.4×10^{-12}	5.80×10^{-13}	6.9×10^{-12}	3.95×10^{-12}
$0 \rightarrow 11$	7.6×10^{-12}	1.97×10^{-13}	7.6×10^{-12}	1.75×10^{-12}
$0 \rightarrow 12$	3.8×10^{-12}	4.34×10^{-14}	3.3×10^{-12}	8.97×10^{-13}

TABLE II. Comparison of rotational rate coefficients from the ground rotational state computed by Wolkovitch *et al.*[25] and in this work.

rate coefficients for high ΔN at 10 K were the source of the differences on the fine structure-resolved rate coefficients exhibited in Fig. 7, then they should vanish or at least decrease at 20 K, where the discrepancies between rotational rate coefficients stay reasonable (below a factor of 5 for all considered transitions). However, the distribution of the fine rate coefficients are very similar at both 10 and 20 K, so this hypothesis is disproved.

Such similarity between the two sets of rotational rate coefficients is not surprising because the PES for both molecular systems (CCS-He vs. OCS-H_2) are similar. Indeed, only the long-range of Green & Chapman[35] OCS-H_2 PES was actually computed with H_2, and all other features of the PES, i.e. the repulsive wall and the potential wells, were computed for the OCS-He system. Therefore, no significant differences were expected between the two sets of rotational rate coefficients for CCS-H_2 and CCS-He. Therefore, the remarkable differences between the fine structure rate coefficients highlighted in Fig. 7 do not seem to originate from the colliders, or from the PES considered. It suggests that the scattering approach is the main reason for such differences.

With the IOS approximation, the exact energy of the fine structure levels are not taken into account in the scattering calculations. Indeed, the later approximation uses rotational cross sections from the ground state to infer fine structure resolved cross sections for all levels considered.[25] However, if CCS energetic structure is not explicitly taken into account, some transitions will be considered as excitations, when, in fact, they are de-excitations such as the $0_1 \rightarrow 1_0$ transition, or all transitions between the 1_1 level and any N_j levels with $N \leq 4$ and $j = N + 1$.

According to these results, the IOS approximation within pure Hund's case (b) for the CCS molecule is failing at reproducing accurate fine-structure resolved rate coefficients at (least at) low temperature. It also suggests that it may fail for other systems with a large spin-splitting as it was already discussed in previous works.[21,25,36,37] Therefore, the conclusions drawn from astrophysical model based on Wolkovitch *et al.*[25] data may need to be reconsidered.

IV. CONCLUSIONS

State-to-state rate coefficients for the CCS($^3\Sigma^-$)-He system were obtained for the 5 - 50 K temperature range, by explicitly taking into account the CCS fine structure. For that purpose, the first PES of the CCS-He van der Waals complex was computed. It exhibits a strong anisotropy, and thus, a great number of *ab initio* points and v_λ(R) coefficients were required to correctly describe it. The dissociation energy of the complex was computed with and without considering explicitly the CCS fine-structure in the Close-Coupling calculations, and the effect of such peculiar structure on this dissociation energy appear to be not huge although not negligible.

Based on the PES, cross sections were computed with the Close-Coupling approach within the intermediate coupling scheme, and rate coefficients for temperature from 5 to 50 K were derived by integration of the cross sections over kinetic energies. Propensity rules were discussed, and the degree of mixing between pure Hund's case (b) basis was found to have a strong influence on them. Therefore, it was concluded that CCS collisional data could only be properly described with the intermediate coupling scheme.

The obtained rate coefficients were compared at 10 and 20 K to previous ones provided by Wolkovitch *et al.*,[25] and a global difference of a factor 2-10 was observed. Some transitions exhibited discrepancies up to 2 orders of magnitudes. Thus, the derived abundances of CCS and extended conclusions might need to be reconsidered.

For now, CCS abundances in astrophysical media were derived within the local thermodynamic approximation (LTE) approximation, which is known to not be accurate in many astrophysical media (such as molecular clouds, where CCS is widely detected) or with the data of Wolkovitch *et al.*[25] With the new set of data provided here, the CCS abundances may be significantly revised, and then, its correlated abundance with HC_3N and carbon chains in general can be further investigated and may decipher on the formation path of such molecules.

ACKNOWLEDGEMENTS

We acknowledge financial support from the European Research Council (Consolidator Grant COLLEXISM, Grant Agreement No. 811363) and the Programme National "Physique et Chimie du Milieu Interstellaire" (PCMI) of CNRS/INSU with INC/INP cofunded by CEA and CNES. We also acknowledge Rennes Metropole for financial support. F.L. acknowledges the Institut Universitaire de France.

CONFLICTS OF INTEREST

The authors have no conflicts to disclose.

SUPPLEMENTARY MATERIAL

A Fortran subroutine of the potential energy surface is available as the supplementary material.

DATA AVAILABILITY

The data that support the findings of this study are available from the corresponding author upon reasonable request.

[1] H. Suzuki, N. Kaifu, T. Miyaji, M. Morimoto, M. Ohishi, and S. Saito, Astrophys. J. **282**, 197 (1984).
[2] N. Kaifu, H. Suzuki, M. Ohishi, T. Miyaji, S.-I. Ishikawa, T. Kasuga, M. Morimoto, and S. Saito, Astrophys. J. **317**, L111 (1987).
[3] S. Saito and K. Kawaguchi, Astron. Astrophys. **317**, L115 (1987).
[4] S. Yamamoto, S. Saito, K. Kawaguchi, Y. Chikada, H. Suzuki, N. Kaifu, S.-I. Ishikawa, and M. Ohishi, Astrophys. J. **361**, 318 (1990).
[5] S. Yamamoto, S. Saito, K. Kawaguchi, N. Kaifu, and H. Suzuki, Astrophys. J. **317**, L119 (1987).
[6] J. Cernicharo, M. Guélin, H. Hein, and C. Kahane, Astron. Astrophys. **181**, 4 (1987).
[7] J. Cernicharo, C. Cabezas, M. Agúndez, B. Tercero, J. R. Pardo, N. Marcelino, J. D. Gallego, F. Tercero, J. A. López-Pérez, and P. de Vicente, Astron. Astrophys. **648**, L3 (2021).
[8] M. Agúndez, J. Cernicharo, and M. Guélin, Astron. Astrophys. **570**, A45 (2014).
[9] M. B. Bell, L. W. Avery, and P. A. Feldman, Astrophys. J. **417**, L37 (1993).
[10] D. Smith, N. G. Adams, K. Giles, and E. Herbst, Astron. Astrophys. **200**, 191 (1988).
[11] H. Suzuki, M. Ohishi, N. Kaifu, T. Kasuga, S.-i. Ishikawa, and T. Miyaji, Vistas in Astronomy **31**, 459 (1988).
[12] T. J. Millar and E. Herbst, Astron. Astrophys. **231**, 466 (1990).
[13] D. A. Howe and T. J. Millar, Mon. Not. R. Astron. Soc. **244**, 444 (1990).
[14] H. Suzuki, S. Yamamoto, M. Ohishi, N. Kaifu, S.-I. Ishikawa, Y. Hirahara, and S. Takano, Astron. Astrophys. **392**, 551 (1992).
[15] S. Petrie, Monthly Notices of the Royal Astronomical Society **281**, 666 (1996).
[16] J. R. Flores, C. M. Estévez, L. Carballeira, and I. P. Juste, J. Chem. Phys. **105**, 4716 (2001).
[17] T. J. Millar, J. R. Flores, and A. J. Markwick, Mon. Not. R. Astron. Soc. **327**, 1173 (2001).
[18] R. I. Kaiser, M. Yamada, and Y. Osamura, J. Chem. Phys. **106**, 4825 (2002).
[19] M. Yamada, Y. Osamura, and R. I. Kaiser, Astron. Astrophys. **395**, 1031 (2002).
[20] N. Sakai, M. Ikeda, M. Morita, T. Sakai, S. Takano, Y. Osamura, and S. Yamamoto, Astrophys. J. **663**, 1174 (2007).
[21] A. Fuente, J. Cernicharo, A. Barcia, and Gómes-Gonzáles, Astron. Astrophys. **231**, 151 (1990).
[22] W. M. Irvine, L. W. Avery, P. Friberg, H. E. Matthews, and L. M. Ziurys, Astro. Lett. Commun. **26**, 167 (1988).
[23] Y. Hirahara, H. Suzuki, S. Yamamoto, K. Kawaguchi, N. Kaifu, M. Ohishi, S. Takano, S.-I. Ishikawa, and A. Masuda, Astrophys. J. **394**, 539 (1992).
[24] T. Velusamy, T. B. H. Kuiper, and W. D. Langer, Astrophys. J. **451**, L75 (1995).
[25] D. Wolkovitch, W. D. Langer, P. F. Goldsmith, and M. Heyer, Astrophys. J. **477**, 241 (1997).
[26] R. Peng, W. D. Langer, T. Velusamy, T. B. H. Kuiper, and S. Levin, Astrophys. J. **497**, 842 (1998).
[27] P. J. Benson, P. Caselli, and P. C. Myers, Astrophys. J. **506**, 743 (1998).
[28] K. Dobashi, T. Shimoikura, T. Ochiai, F. Nakamura, S. Kameno, I. Mizuno, and K. Taniguchi, Astrophys. J. **879**, 88 (2019).
[29] J. H. He, Dinh-V-Trung, S. Kwok, H. S. P. Müller, Y. Zhang, T. Hasegawa, T. C. Peng, and Y. C. Huang, Astrophys. J., Suppl. Ser. **177**, 275 (2008).
[30] F. Scappini and C. Codella, Mon. Not. R. Astron. Soc. **282**, 587 (1996).
[31] S. M. Levin, W. D. Langer, T. Velusamy, and T. B. H. Kuiper, Astrophys. J. **555**, 850 (2001).
[32] K. I. Uchida, D. Fiebig, and R. Güsten, Astron. Astrophys. **371**, 274 (2001).
[33] E. Roueff and F. Lique, Chem. Rev. **113**, 8906 (2013).
[34] M. H. Alexander and P. J. Dagdigian, J. Chem. Phys. **79**, 302 (1983).
[35] S. Green, Astrophys. J., Suppl. Ser. **37**, 26 (1978).
[36] F. Lique, A. Spielfiedel, M.-L. Dubernet, and N. Feautrier, J. Chem. Phys. **123**, 134316 (2005).
[37] F. Lique, M.-L. Dubernet, A. Spielfiedel, and N. Feautrier, Astron. Astrophys. **450**, 399 (2006).
[38] A. Murakami, Astrophys. J. **357**, 288 (1990).
[39] Y. Xie and H. F. Schaefer, J. Chem. Phys. **96**, 3751 (1992).
[40] M. J. Deegan and P. J. Knowles, Chem. Phys. Lett. **227**, 321 (1994).
[41] S. M. Cybulski and R. R. Toczyłowski, J. Chem. Phys. **111**, 10520 (1999).
[42] Werner, "Molpro, a package of ab initio programs, version 2015.1, 2015,".
[43] S. Boys and F. Bernardi, Mol. Phys. **19**, 553 (1970).
[44] H.-J. Werner, B. Follmeg, and M. H. Alexander, J. Chem. Phys. **89**, 3139 (1988).
[45] J. B. Tatum and J. K. G. Watson, Can. J. Phys. **49**, 2693 (1971).
[46] G. C. Corey, M. H. Alexander, and J. Schaefer, J. Chem. Phys. **85**, 2726 (1986).
[47] B. A. McGuire, M.-A. Martin-Drumel, K. L. K. Lee, J. F. Stanton, C. A. Gottlieb, and M. C. McCarthy, Phys. Chem. Phys. Chem. **20**, 13870 (2018).
[48] D. E. Manolopoulos, J. Chem. Phys. **85**, 6425 (1986).
[49] J. Hutson, "BOUND computer code, version 5, distributed by Collaborative Computational Project No.6 of the Science and Engineering Research Council," (1993).
[50] E. A. Bergin and M. Tafalla, Annu. Rev. Astron. Astrophys. **45**, 339 (2007).
[51] J. Hutson and S. Green, "Molscat computer program, version 14, distributed by Collaborative Computational Projet No. 6 of the UK Science and Engineering Research Council," (1994).
[52] M. Costes and C. Naulin, Chem. Sci. J. **7**, 2462 (2016).
[53] T. Orlikowski, Mol. Phys. **56**, 35 (1985).
[54] F. Lique, M.-L. Senent, A. Spielfiedel, and N. Feautrier, J. Chem. Phys. **126**, 164312 (2007).
[55] F. Lique, J. Chem. Phys. **132**, 044311 (2010).
[56] R. Ramachandran, J. Kłos, and F. Lique, J. Chem. Phys. **148**, 084311 (2018).
[57] S. Green, Astron. Astrophys. **434**, 188 (1994).
[58] R. Toboła, F. Dumouchel, J. Kłos, and F. Lique, J. Chem. Phys. **134**, 024305 (2011).
[59] F. Dumouchel, J. Kłos, R. Toboła, A. Bacmann, S. Maret, P. Hily-Blant, A. Faure, and F. Lique, J. Chem. Phys. **137**, 114306 (2012).
[60] G. C. Corey and F. R. McCourt, J. Chem. Phys. **87**, 2723 (1983).

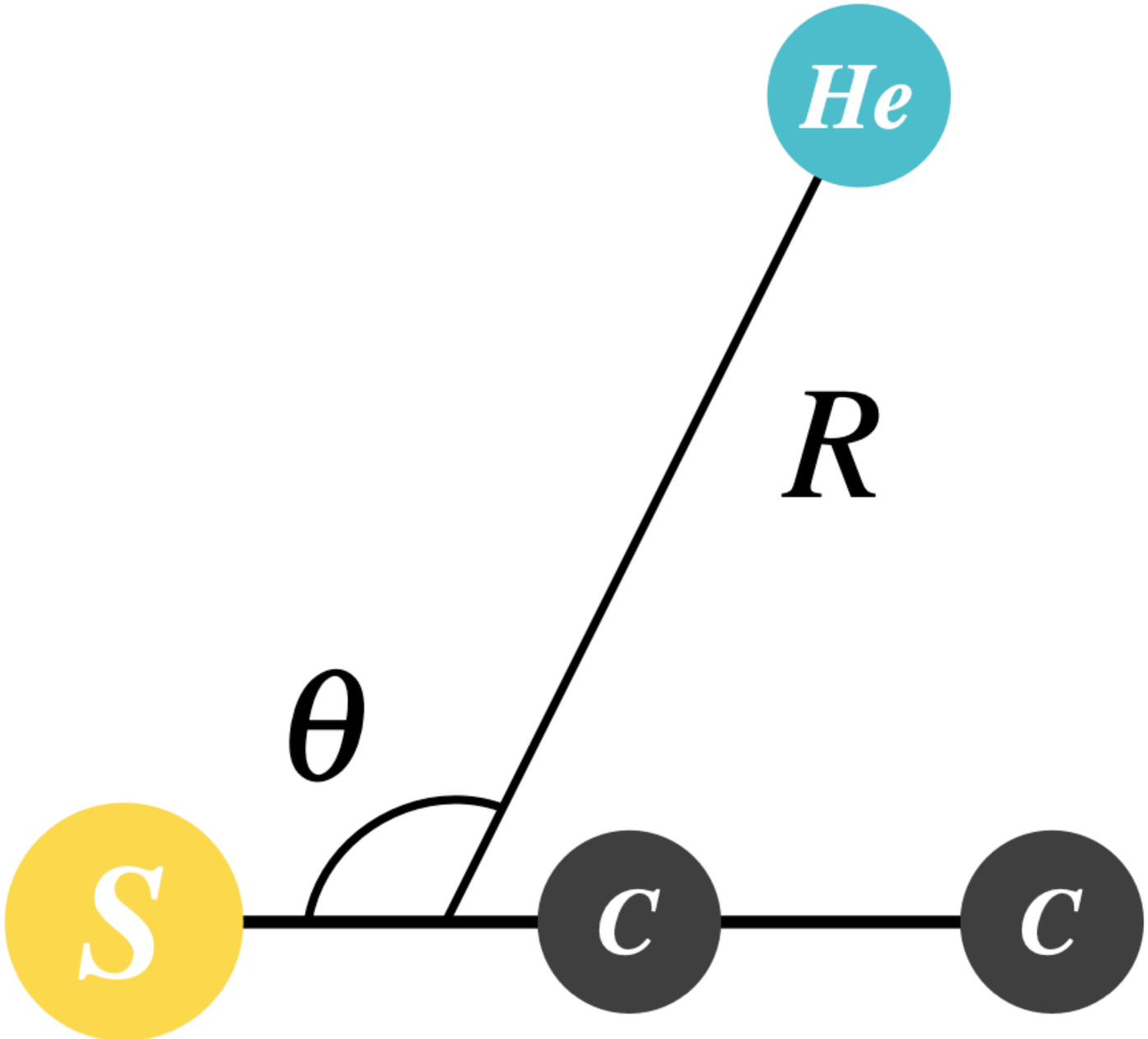
He
R
θ
S
C
C

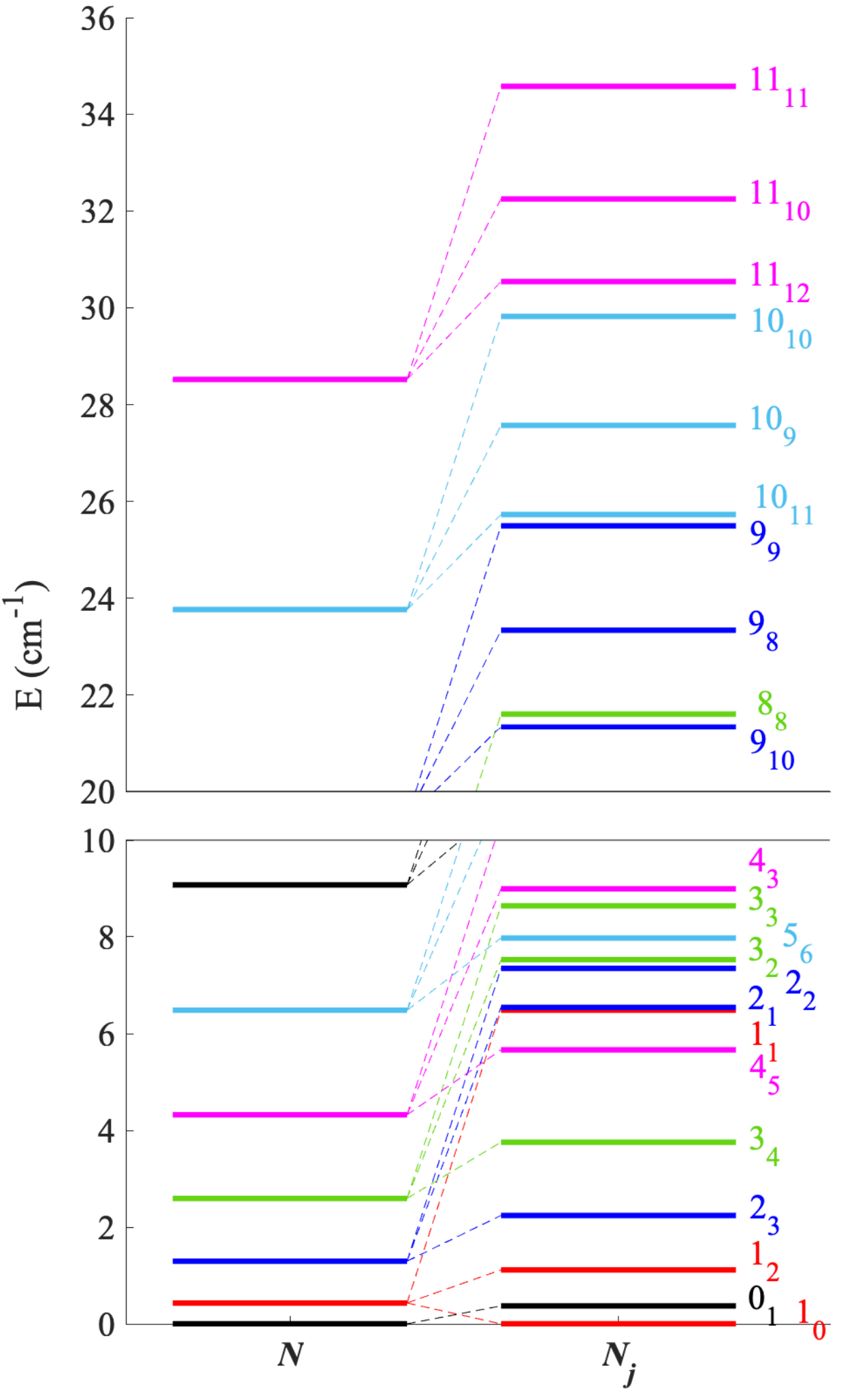
E (cm-1)
36
34
32
30
28
26
24
22
20
10
8
6
4
2
0
N
Nj
11 11
11 10
11 12
10 10
10 9
10 11
9 9
9 8
8 8
9 10
4 3
3 3
5 6
3 2
2 2
2 1
1 1
4 5
3 4
2 3
1 2
0 1
1 0

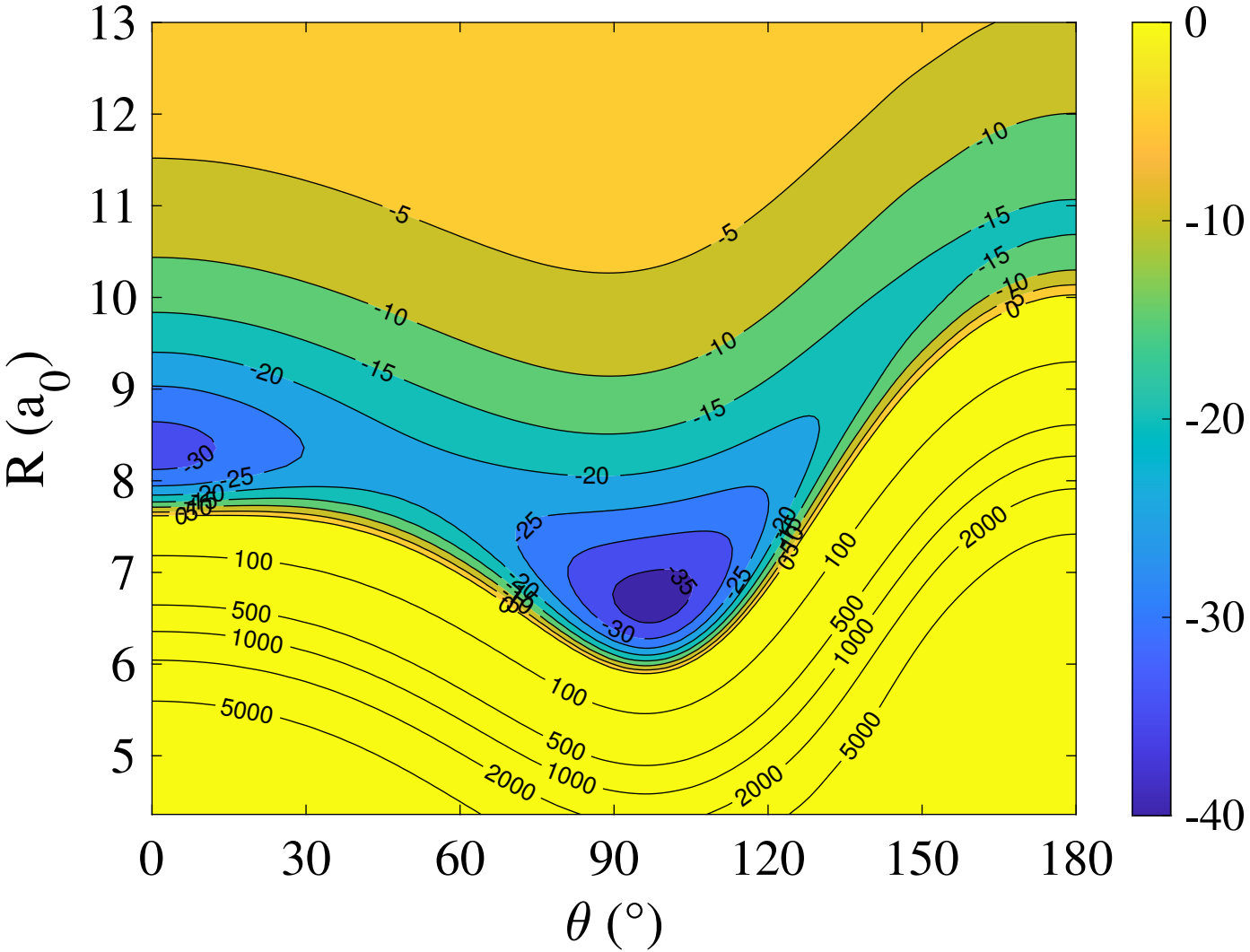
R (a_0)
θ (°)
13
12
11
10
9
8
7
6
5
0
30
60
90
120
150
180
0
-10
-20
-30
-40

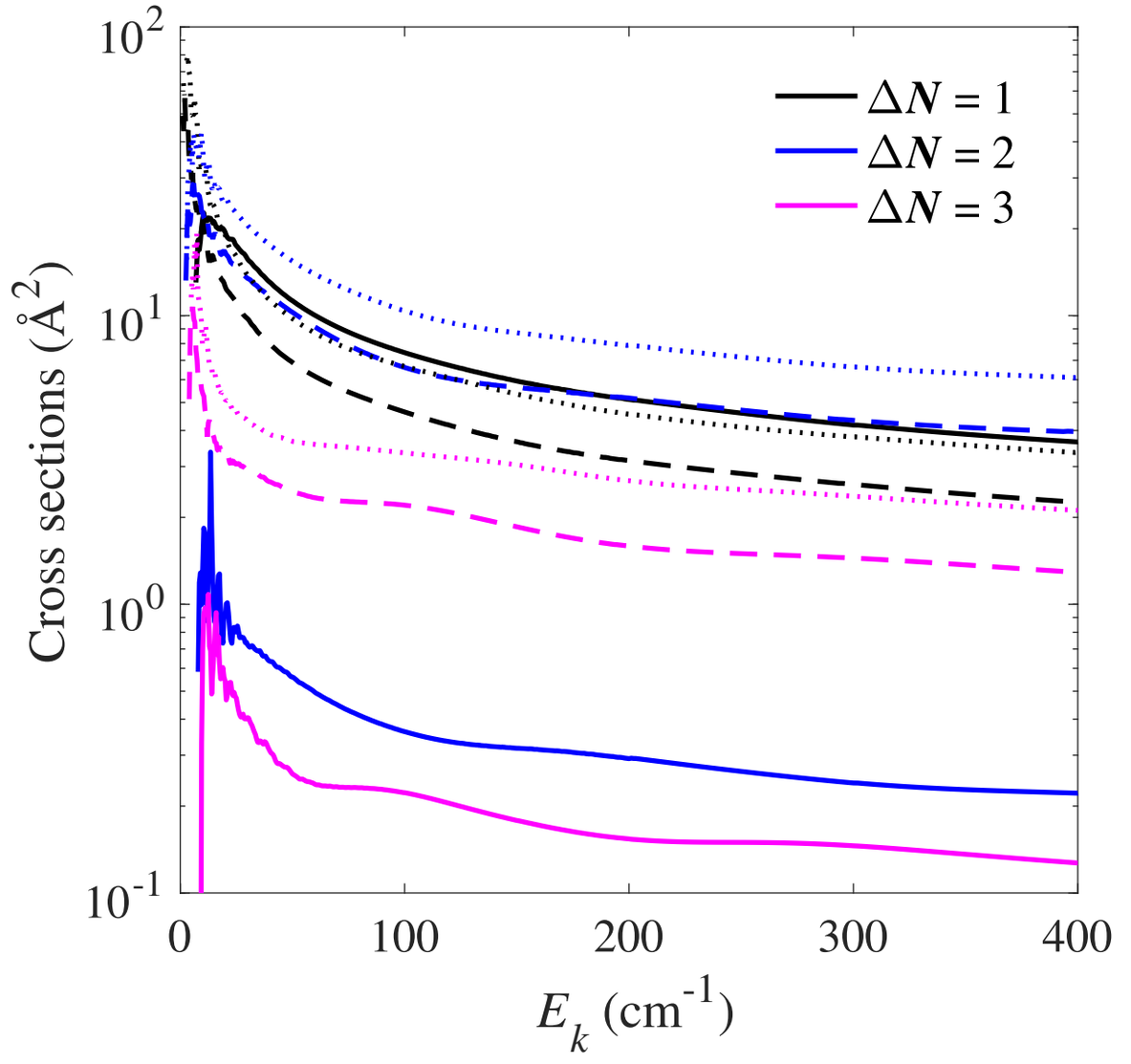
10^2
10^1
10^0
10^{-1}
Cross sections (Å^2)
$\Delta N = 1$
$\Delta N = 2$
$\Delta N = 3$
0
100
200
300
400
E_k (cm^{-1})

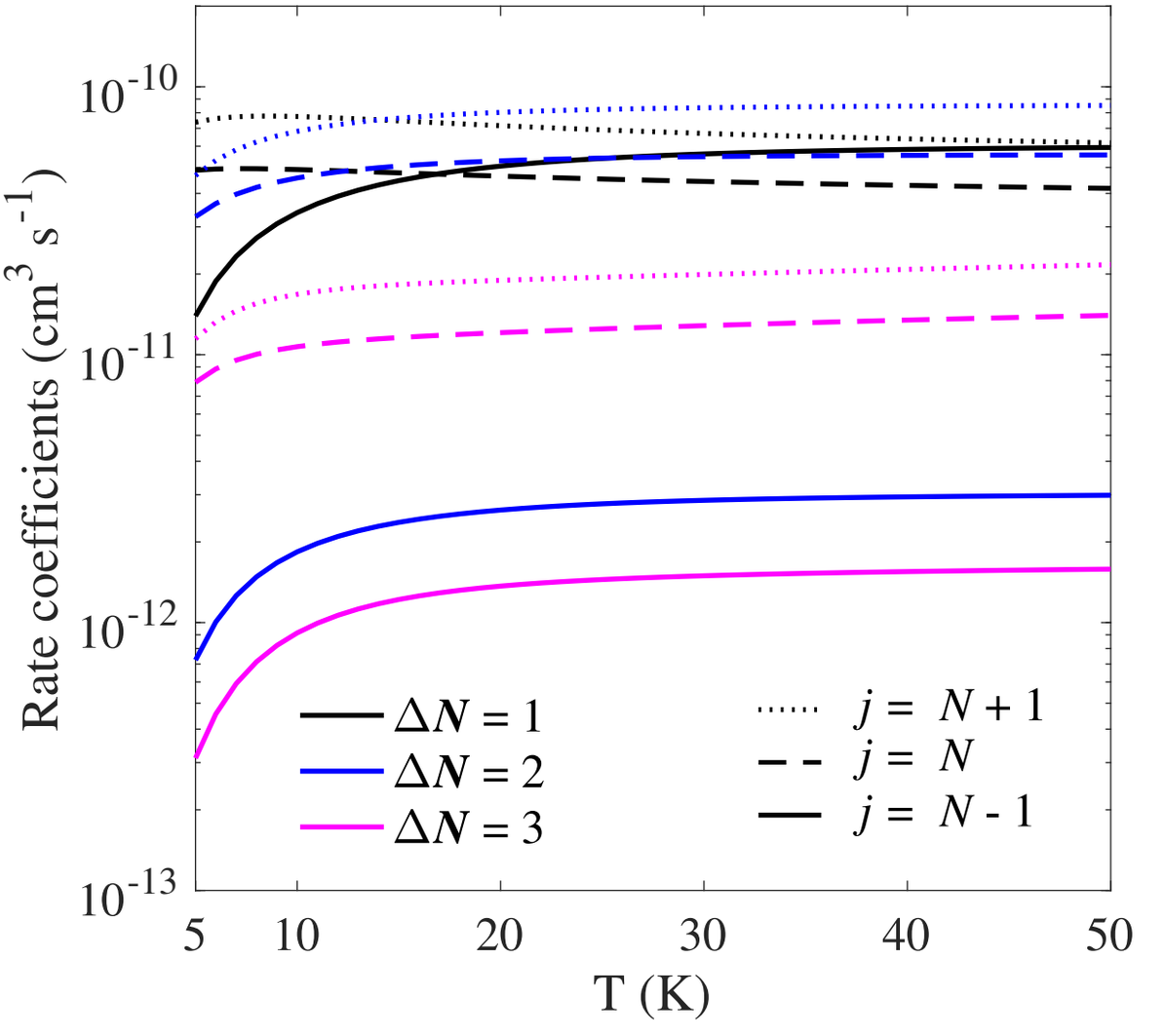
10^{-10}
10^{-11}
10^{-12}
10^{-13}
Rate coefficients (cm^3 s^{-1})
$\Delta N = 1$
$\Delta N = 2$
$\Delta N = 3$
$j = N + 1$
$j = N$
$j = N - 1$
5
10
20
30
40
50
T (K)

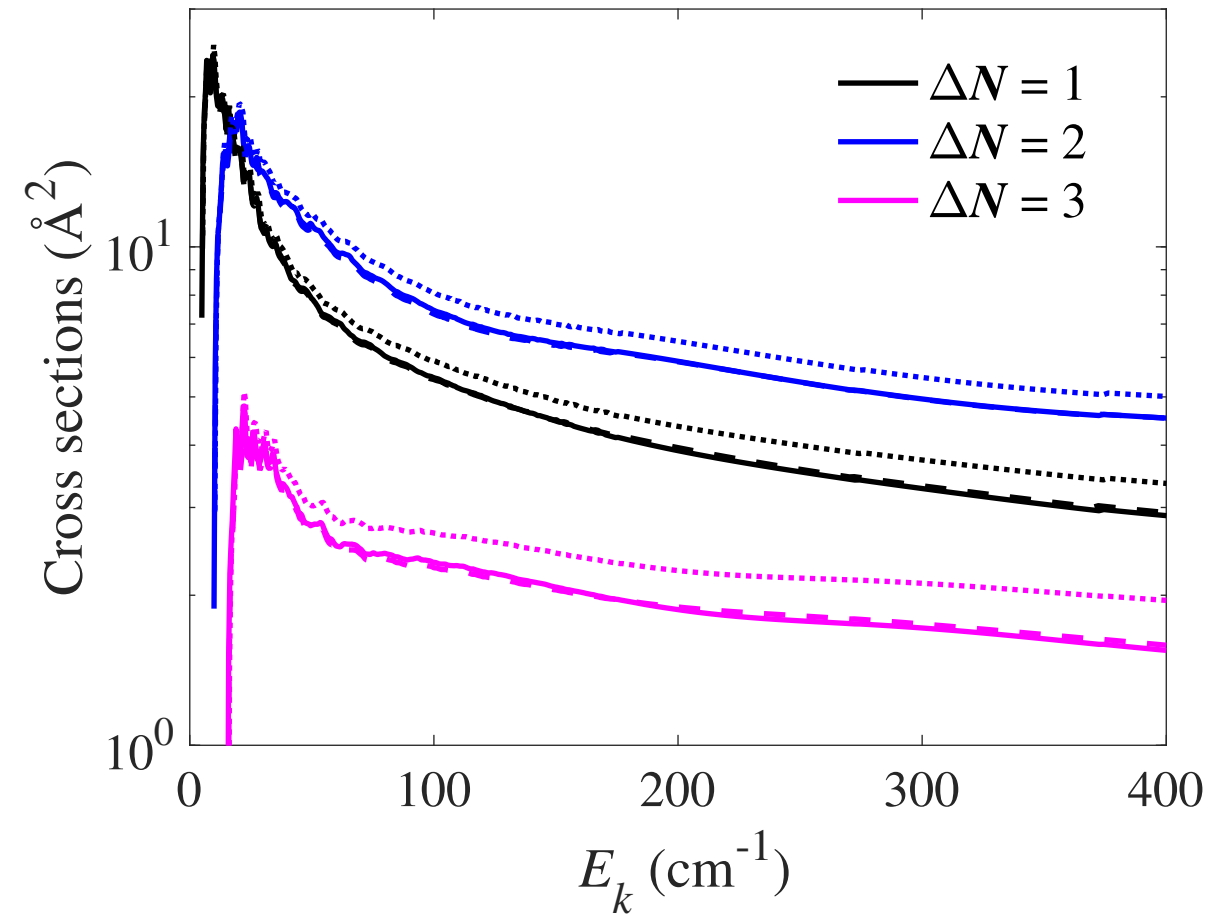
Cross sections (Å^2)
10^1
10^0
0
100
200
300
400
E_k (cm^{-1})
$\Delta N = 1$
$\Delta N = 2$
$\Delta N = 3$

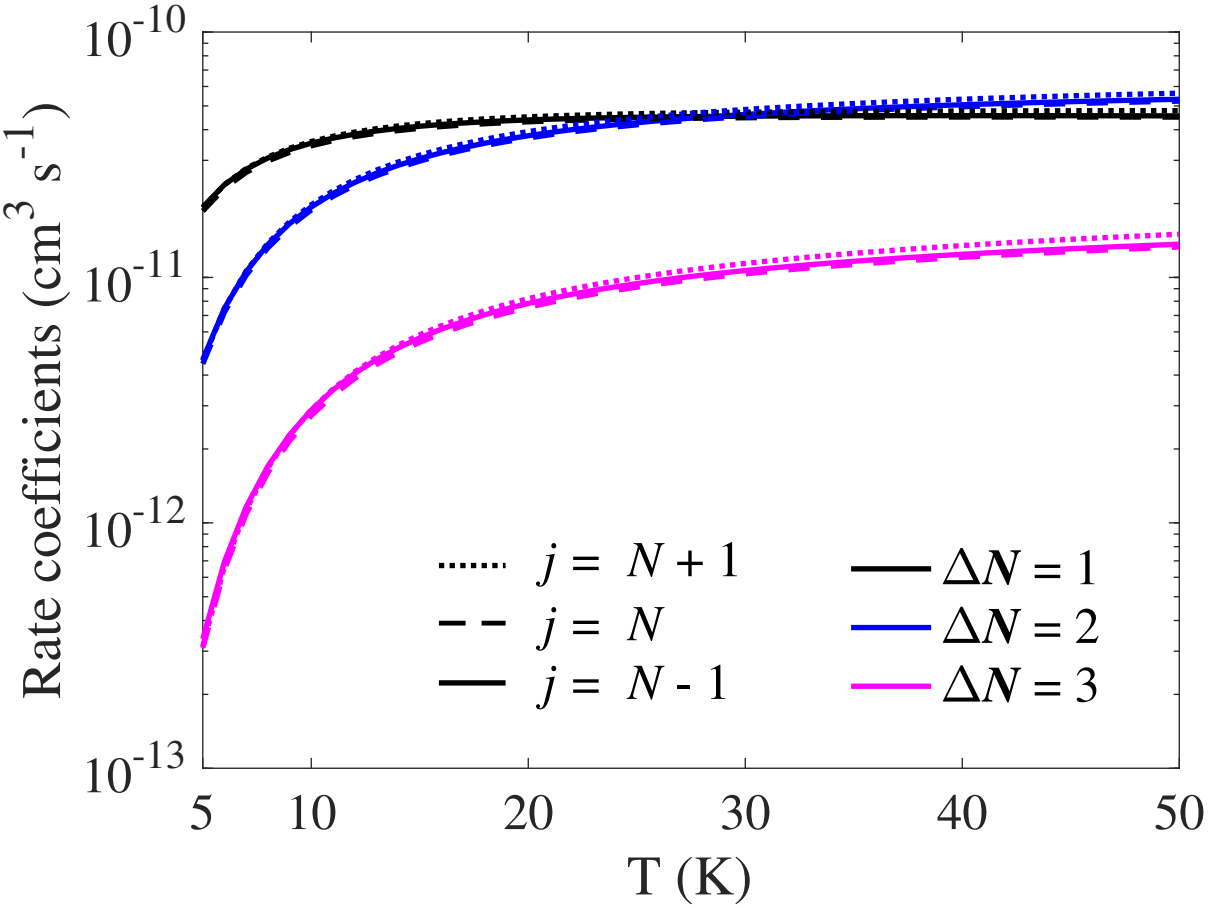
Rate coefficients (cm^3 s^{-1})
10^{-10}
10^{-11}
10^{-12}
10^{-13}
5
10
20
30
40
50
T (K)
$j = N + 1$
$j = N$
$j = N - 1$
$\Delta N = 1$
$\Delta N = 2$
$\Delta N = 3$

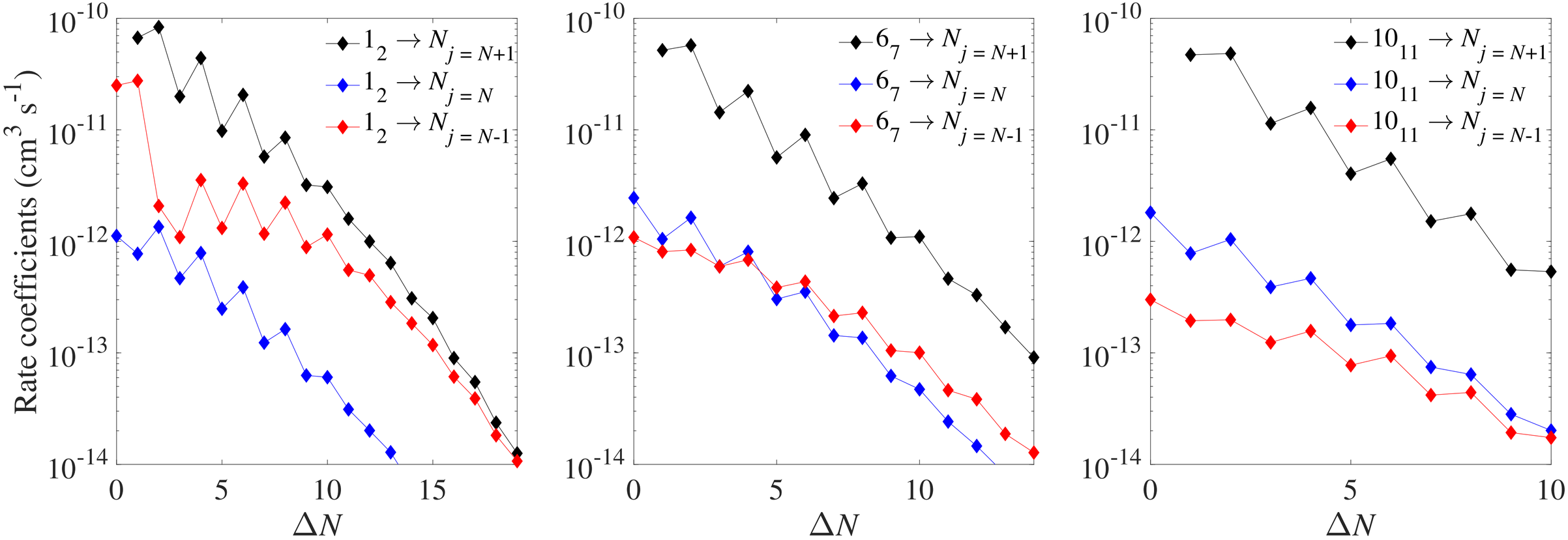
Rate coefficients (cm^3 s^{-1})
10^{-10}
10^{-11}
10^{-12}
10^{-13}
10^{-14}
0
5
10
15
ΔN
$1_2 \rightarrow N_{j=N+1}$
$1_2 \rightarrow N_{j=N}$
$1_2 \rightarrow N_{j=N-1}$
$6_7 \rightarrow N_{j=N+1}$
$6_7 \rightarrow N_{j=N}$
$6_7 \rightarrow N_{j=N-1}$
$10_{11} \rightarrow N_{j=N+1}$
$10_{11} \rightarrow N_{j=N}$
$10_{11} \rightarrow N_{j=N-1}$

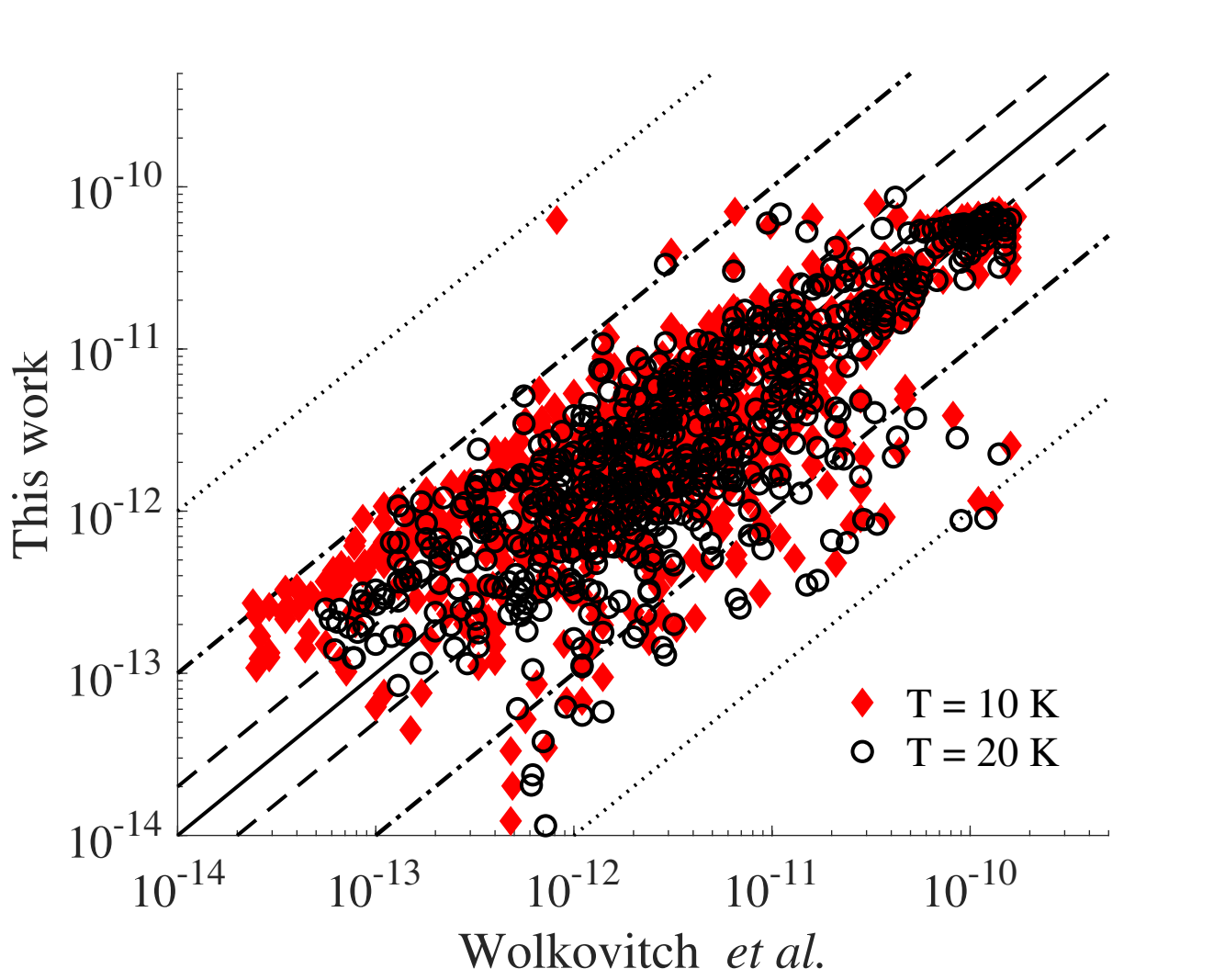
This work
Wolkovitch *et al.*
10^{-10}
10^{-11}
10^{-12}
10^{-13}
10^{-14}
10^{-14}
10^{-13}
10^{-12}
10^{-11}
10^{-10}
T = 10 K
T = 20 K